LETTERS

Multiple native states reveal persistent ruggedness of an RNA folding landscape

Sergey V. Solomatin[1], Max Greenfeld[2], Steven Chu[3,4]† & Daniel Herschlag[1]

According to the 'thermodynamic hypothesis', the sequence of a biological macromolecule defines its folded, active (or 'native') structure as a global energy minimum in the folding landscape[1,2]. However, the enormous complexity of folding landscapes of large macromolecules raises the question of whether there is in fact a unique global minimum corresponding to a unique native conformation or whether there are deep local minima corresponding to alternative active conformations[3]. The folding of many proteins is well described by two-state models, leading to highly simplified representations of protein folding landscapes with a single native conformation[4,5]. Nevertheless, accumulating experimental evidence suggests a more complex topology of folding landscapes with multiple active conformations that can take seconds or longer to interconvert[6–8]. Here we demonstrate, using single-molecule experiments, that an RNA enzyme folds into multiple distinct native states that interconvert on a timescale much longer than that of catalysis. These data demonstrate that severe ruggedness of RNA folding landscapes extends into conformational space occupied by native conformations.

Biopolymers face the challenge of folding a linear chain into complex three-dimensional conformations that have specific biological activities. According to the thermodynamic hypothesis, sequences of biological macromolecules have evolved to specify the active conformation as a minimum in free energy, ensuring that native states are more stable than an ensemble of all possible inactive conformations[1]. In the language of folding landscapes, the native conformation is the global energy minimum, separated from an ensemble of inactive conformations by a large energy gap[2–4]. However, the enormous complexity of the conformational space of a typical macromolecule—there are at least 10^{30} conformations for a small protein containing 100 amino acids[9]—raises the question of whether such energy minima are unique or whether there are multiple local energy minima that correspond to alternative active conformations. Observations of hysteresis in enzyme kinetics and of kinetic complexities in protein folding and unfolding and protein–ligand binding provided early evidence that some protein enzymes can exist in several catalytically active forms[6,10]. In the past decade, single-molecule experiments have provided additional evidence for multiple active conformers that slowly interconvert[11–13].

Functional RNAs represent a chemically distinct class of biopolymers that face a folding problem analogous to that of proteins. RNA folding landscapes have long been considered more rugged than protein landscapes[14–16], owing to the limited information content of RNA primary structure and the high stability of RNA secondary structures. Observations of very long timescales for folding and the occurrence of multiple, long-lived intermediates appear to support these views[15,17]. It is not known, however, whether ruggedness extends into the region of the native state, resulting in multiple active conformations. Experiments with a small catalytically active RNA, the hairpin ribozyme, revealed several distinct active forms of these molecules[18,19]. Although these results are suggestive of landscape ruggedness, there is insufficient evidence to demonstrate that distinct forms are interconverting conformations, and the results leave open the possibility that covalent differences exist between the molecules that had different behaviour.

We have used single-molecule fluorescence resonance energy transfer (FRET) experiments to test whether the *Tetrahymena* group I ribozyme, a large, efficient RNA catalyst, folds into a unique native conformation or into multiple native conformations. Our results provide strong evidence for multiple conformations of the native state that interconvert but are separated by large energetic barriers.

The *Tetrahymena* group I ribozyme is a ~400-nucleotide RNA enzyme that folds in the presence of Mg^{2+} into an active form that catalyses cleavage of an oligonucleotide substrate by an exogenous guanosine nucleophile. Binding of the oligonucleotide substrate to the folded ribozyme occurs in two steps (Fig. 1). In the first step, the substrate binds to a single-stranded 5′-end region, forming the P1 duplex. In the second step, the P1 duplex docks into tertiary interactions in the active site[20,21].

We tested whether the ribozyme is folded into a single native conformation by measuring the thermodynamics and kinetics of docking for individual molecules using single-molecule FRET. If all

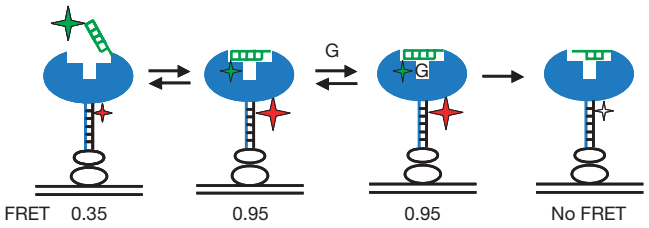

Figure 1 | Docking and cleavage of the oligonucleotide substrate by the *Tetrahymena* ribozyme, observed using single-molecule FRET. The ribozyme is shown in blue, the P1 duplex is shown in green and a DNA tether base-paired to a 3′-end extension of the ribozyme is shown in black. Streptavidin and biotinylated bovine serum albumin are used for surface attachment of the construct and are shown as clear ovals. The substrate is labelled with the FRET donor (Cy3 dye, green star) and the DNA tether is labelled with the FRET acceptor (Cy5 dye, red and white stars). The relative sizes of the stars indicate the relative fluorescence intensities of the dyes. Donor fluorescence is excited using the 532-nm laser. The FRET efficiency fluctuates between the levels of 0.35 in the open complex and 0.95 in the closed complex, as shown. After guanosine (G) binds, the substrate is cleaved and the Cy3-labelled 3′-end rapidly dissociates, leading to loss of Cy5 fluorescence, as indicated by the white star, and the absence of FRET[27].

[1]Department of Biochemistry, [2]Department of Chemical Engineering, Stanford University, Stanford, California 94305, USA. [3]Lawrence Berkeley National Laboratory, Berkeley, California 94720, USA. [4]Department of Physics and Molecular and Cell Biology, University of California, Berkeley, California 94720, USA. †Present address: United States Department of Energy, Washington DC 20585, USA.

of the molecules were folded to a single native conformation, the docking behaviour for each single molecule would be identical to the ensemble average behaviour. However, individual ribozyme molecules from a single sample that were folded together and observed side by side under identical conditions instead displayed a broad distribution of docking behaviours (Fig. 2). For example, the docking equilibrium constants for the molecules in Fig. 2a–d vary by a factor of 300.

The accuracy of measuring docking equilibria from single-molecule FRET traces is limited by the finite length of each trace, caused by photobleaching. Therefore, a distribution of docking behaviours is expected even if all of the molecules are in the same conformation. Quantitative modelling of this effect (Supplementary Figs 1 and 2) demonstrated that the finite lengths can account for only a small fraction of the width of the observed distribution. More than six conformations with different docking thermodynamics are needed to account for this distribution (Fig. 2e and Supplementary Fig. 3). The docking and undocking rate constants determined for individual molecules also vary across a broad distribution (Fig. 2f) without discernable clustering into subgroups that might indicate a small number of distinct conformations.

A simple model that could account for the multiple docking states suggests that some of the observed molecules represent partially folded forms of the ribozyme that are capable of docking but have not reached the native state. To test this possibility, we determined the catalytic activity of molecules across the broad range of docking behaviours. We first measured the docking equilibrium for each molecule and then induced cleavage by adding guanosine to allow chemical catalysis to occur (Fig. 1). The proportion of molecules in which the substrate was uncleaved decayed mono-exponentially with an end point of 6%, indicating that 94% of the molecules were catalytically active and that only 6% were inactive or had much lower activity. Furthermore, nearly all of the molecules throughout the distribution of docking conformations were catalytically active (Supplementary Table 1).

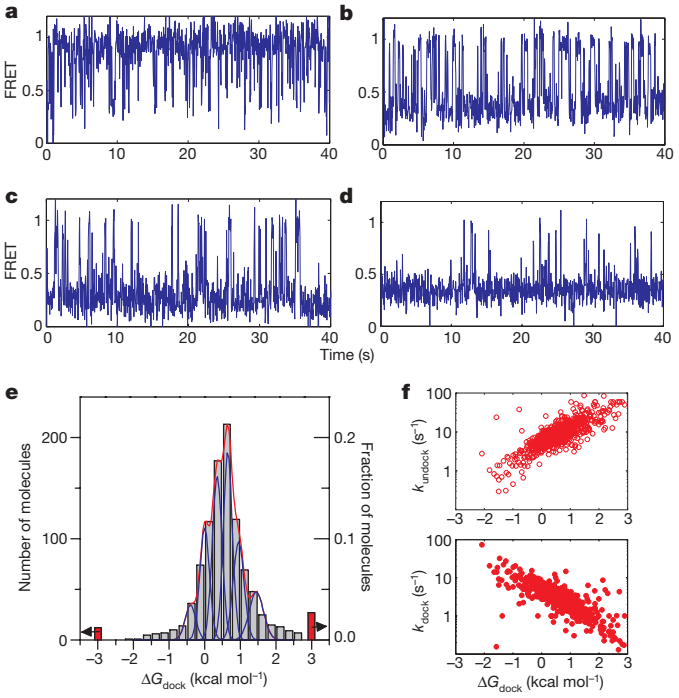

Figure 2 | Distribution of docking behaviours of individual ribozyme molecules. **a**–**d**, Representative examples of FRET traces, which give docking equilibria of $K_{dock} = 8$ (**a**), 0.5 (**b**), 0.08 (**c**) and 0.03 (**d**), corresponding to docking free-energy values of $\Delta G_{dock} = -1.4$, 0.4, 1.4 and 2.0 kcal mol^{-1}, respectively. **e**, The distribution of docking behaviours of individual ribozyme molecules (grey bars). Red bars correspond to molecules that displayed no docking or no undocking transitions, for which only the limits of ΔG_{dock} could be determined (as indicated by arrows). Blue peaks show the expected distribution widths for individual docking conformations (Supplementary Information). The red line shows the best fit of the distribution to a sum of distributions from six docking conformations. **f**, Docking (k_{dock}) and undocking (k_{undock}) rate constants of individual molecules. Experiments were performed in a standard buffer containing 10 mM $MgCl_2$ at 22 °C. The substrate oligonucleotide was CCCUC(2′-methoxyU)AAACC-Cy3.

We next determined whether molecules in different docking conformations, as assessed by their distinct docking equilibria, exhibited the same or distinct cleavage kinetics. We binned molecules with similar docking behaviours (Fig. 3a) and analysed cleavage kinetics within each bin (Fig. 3b and Supplementary Table 1). Both the cleavage rate constant, k_{cleave}, and the end points were similar for all bins, despite the docking equilibria differing among them by a factor of at least 800. Thus, molecules that formed docked states with the same catalytic activity had distinct docking behaviours, providing direct evidence for a heterogeneous native state. Additional experiments suggest that the heterogeneity arises from different molecules forming different subsets of the tertiary docking interactions with the functional groups on the P1 duplex (Supplementary Fig. 4).

Multiple native conformations of the ribozyme observed in our experiments could represent multiple distinct folds of the same sequence, as implicitly assumed above. Alternatively, they could instead represent similar folded states of RNA molecules that have different sequences because of errors in synthesis, unintended chemical modifications or degradation. Covalent heterogeneity of RNA has been considered as a possible origin of multiple conformations of the hairpin ribozyme, although no direct evidence for or against this proposal has been accumulated, and it may be difficult to rule out covalent heterogeneity decisively using assays such as mass spectrometry because modifications can be mass neutral and the formation of multiple modified species each in low abundance can be difficult to detect[19,22].

Stable covalent conformational differences can be distinguished from interconvertible conformational differences if interconversion between different conformations can be observed under some conditions. If each detected 'conformation', or behaviour, can interconvert to others, conformational heterogeneity is strongly suggested, whereas the absence of extensive interconversion under any condition leaves open the possibilities of covalent heterogeneity or extremely stable and long-lived RNA species[23,24].

We determined whether molecules can change their docking behaviour by comparing docking of individual molecules before and after unfolding under mild denaturing conditions. Removing Mg^{2+} using EDTA disrupts the tertiary structure of the ribozyme but leaves most of the secondary structure intact and allows the molecules to remain

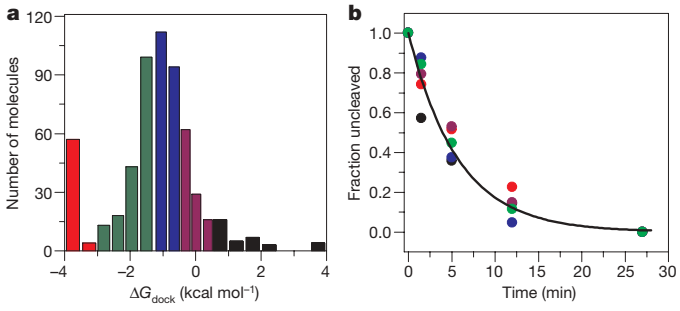

Figure 3 | Catalytic activities of molecules from different parts of docking distribution are the same. **a**, Distribution of docking behaviours was split into five bins marked using different colours. Cleavage experiments were performed with the CCCUC(2′-deoxyU)A-Cy3 substrate oligonucleotide, which docks more stably than the CCCUC(2′-methoxyU)AAACC-Cy3 substrate in Fig. 2. **b**, Cleavage kinetics within each bin were the same as the global average (line indicates global fit). Kinetic parameters for the global fit and fits for individual bins are given in Supplementary Table 1.

tethered to the surface. As illustrated in Fig. 4a, if all molecules quickly interconvert in the unfolded state, each molecule could then refold to any of the docking conformations, independent of which conformation it populated before unfolding. We grouped molecules into three non-overlapping subpopulations on the basis of their docking equilibrium constant before unfolding (Fig. 4b) and compared the distributions of conformations that each molecule populated after refolding. As shown in Fig. 4c, molecules from each of the three original subpopulations had docking behaviours that ranged across the entire distribution. (For traces demonstrating interconversion, see Fig. 4e and Supplementary Fig. 7.) These observations indicate that in the unfolded state all or nearly all of the conformational states can interconvert to any other conformation. Incomplete overlap of the distributions suggests either that some interconversions are slow on the timescale of minutes even in the unfolded state or that covalent differences are present in a subset of the molecules.

The original observation of multiple docking behaviours of active molecules (Figs 2 and 3) indicated that in the folded state the interconversions must be slow relative to the minute timescale of the observations. If interconversions in the folded state were slower than in the unfolded state, it would indicate that the energy landscape becomes more rugged going from the unfolded state to the native state. To address this, we evaluated the extent of interconversion in the folded state. The data in Fig. 4d show that there was little interconversion between docking behaviours even after 40 min; that is, most of the molecules 'remembered' their initial docking equilibria. Nevertheless, some of the molecules changed their docking behaviours during this period (9% of all molecules; Fig. 4d and Supplementary Information). A simple explanation that accounts for the much smaller extent of interconversion in the folded state than in the unfolded state is that the energy barriers separating different conformations are higher in the folded state and the rate of interconversion is hence lower (~100-fold). The data on interconversion under different conditions suggest that the ribozyme folding landscape is moderately rugged in the region occupied by unfolded conformations and becomes more rugged towards the region occupied by the native conformations.

The multiple active conformations of the *Tetrahymena* group I ribozyme offer a glimpse of the full complexity of the folding landscape of a functional RNA. Taken together with the previous evidence for proteins, the results presented here suggest that the complexity of native folded states may be an inherent property of biopolymers.

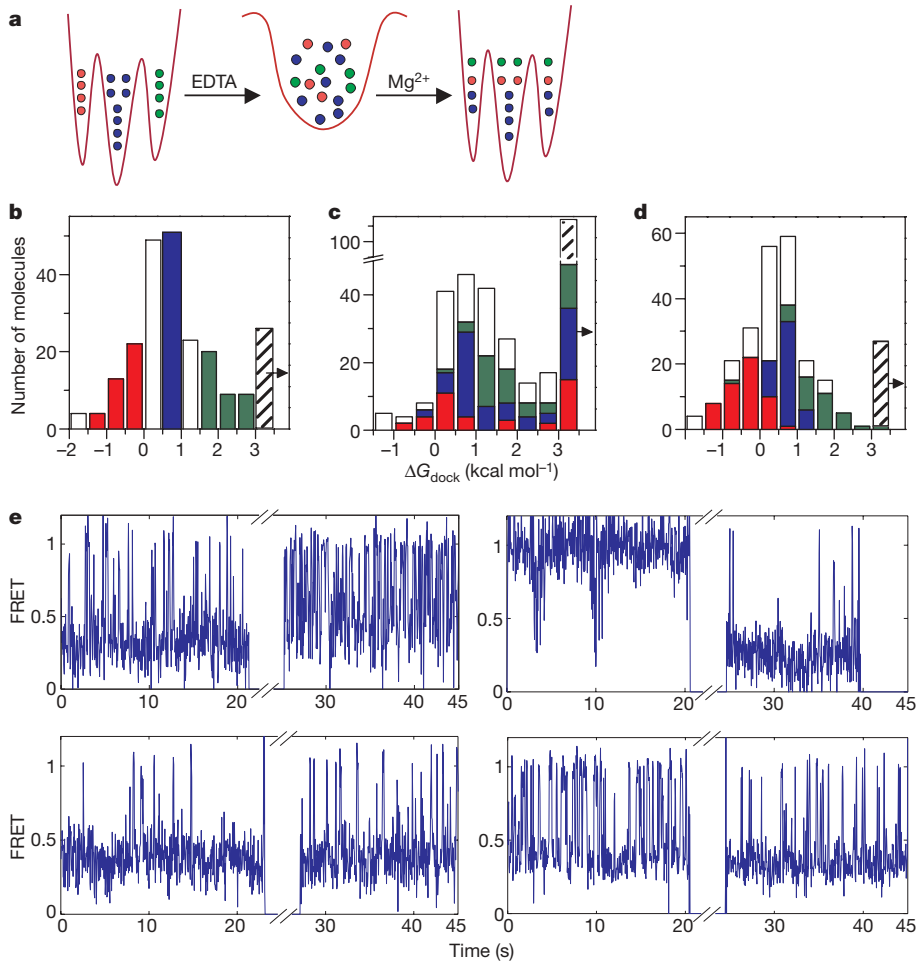

Figure 4 | Interconversion of docking behaviours. **a**, Schematic illustrating changes in docking following fast interconversion in the unfolded state. If interconversions were very slow, each molecule would display the same docking behaviour before and after unfolding. **b**, Distribution of ΔG_{dock} before unfolding. Red, blue and green bars indicate three selected conformations. White bars indicate molecules not included in the analysis to ensure non-overlap of selected conformations. The rightmost bin contains molecules that displayed no docking transitions, for which only the limits of ΔG_{dock} could be determined (as indicated by the arrow). **c**, Distribution of ΔG_{dock} after refolding. The rightmost bin contains mostly misfolded molecules (Supplementary Information)[26,29]. Coloured bars indicate the number of molecules in the correspondingly coloured bins before unfolding (in **b**). **d**, Distribution of ΔG_{dock} after 40 min in the folded state. Coloured bars indicate the number of molecules in the correspondingly coloured bins at the zero time point. The rightmost bin contains molecules that displayed no docking transitions, as in **b**. **e**, Example traces showing interconversions after refolding (see also Supplementary Fig. 7). Breaks in FRET traces correspond to the time spent unfolded. Before and after refolding, the ΔG_{dock} values for the molecules shown were 1.2 and 0.1 (top left), −1.8 and 2.1 (top right), 2.0 and 1.2 (bottom left), and 0.4 and 1.5 kcal mol^{-1} (bottom right), and the *P* values indicating the significance level for interconversion were 0.01, 10^{-15}, 0.1 and 0.1, respectively.

These observations prompt us to revisit the Levinthal paradox in a different context. Levinthal noted that proteins cannot sample all of conformational space on a biological timescale, leading to the notion that there must be a preferred pathway to the native state[25]. More recent work has emphasized the likelihood of there being multiple pathways to the folded state of proteins and RNAs. Multiple pathways, combined with limitations to full sampling, may lead to multiple 'end points', that is, multiple native-state local minima. This picture, although counter to traditional viewpoints, has some support in the protein-folding literature and is strongly supported for the *Tetrahymena* group I RNA by this and previous[26] folding studies. We further speculate that perhaps folded RNAs or proteins in different conformations may respond to cellular or environmental cues in different ways and contribute to stochastic diversity.

METHODS SUMMARY

We synthesized the L-16 form of the *Tetrahymena* group I ribozyme, extended at the 3′-end by a 26-nucleotide T2 tail, by *in vitro* transcription, and purified it by denaturing polyacrylamide gel electrophoresis. Oligonucleotides were obtained commercially (Integrated DNA Technologies and Dharmacon), fluorescently labelled and purified by denaturing polyacrylamide gel electrophoresis. We bound the DNA tether to the ribozyme by annealing (heating at 95 °C for 3 min; cooling to 50 °C at 0.1 °C s^{-1}) and then folding in 10 mM $MgCl_2$ (30 min at 50 °C).

The oligonucleotide substrates were bound to the tether-bound, prefolded ribozyme at 1 μM concentration (10 min at 22 °C). The ribozyme was then diluted to 30–100 pM final concentration for deposition on slides coated with BSA-biotin/streptavidin, as described[27]. Single-molecule FRET experiments were carried out on a home-built prism-based total-internal-reflection microscope, similar to one previously described[28]. Data collection and analysis were performed using home-written programs in C++ and MATLAB R2008a (Mathworks). Details of the methods, including sample preparation, data collection and analysis, and numerical simulations, are presented in full Methods.

Full Methods and any associated references are available in the online version of the paper at www.nature.com/nature.

Received 1 July; accepted 27 November 2009.

1. Anfinsen, C. B. Principles that govern the folding of protein chains. *Science* **181,** 223–230 (1973).
2. Bryngelson, J. D., Onuchic, J. N., Socci, N. D. & Wolynes, P. G. Funnels, pathways and the energy landscape of protein folding: a synthesis. *Proteins Struct. Funct. Genet.* **21,** 167–195 (1995).
3. James, L. C. & Tawfik, D. S. Conformational diversity and protein evolution - a 60-year-old hypothesis revisited. *Trends Biochem. Sci.* **28,** 361–368 (2003).
4. Zwanzig, R. Two-state models of protein folding kinetics. *Proc. Natl Acad. Sci. USA* **94,** 148–150 (1997).
5. Dill, K. A. & Chan, H. S. From Levinthal to pathways to funnels. *Nature Struct. Biol.* **4,** 10–19 (1997).
6. Schmid, F. X. & Blaschek, H. A. Native-like intermediate on the ribonuclease A folding pathway. *Eur. J. Biochem.* **114,** 111–117 (1981).
7. Jennings, P. A., Finn, B. E., Jones, B. E. & Matthews, C. R. A reexamination of the folding mechanism of dihydrofolate reductase from *Escherichia coli*: verification and refinement of a four-channel model. *Biochemistry* **32,** 3783–3789 (1993).
8. Kamagata, K., Sawano, Y., Tanokura, M. & Kuwajima, K. Multiple parallel-pathway folding of proline-free staphylococcal nuclease. *J. Mol. Biol.* **332,** 1143–1153 (2003).
9. Dinner, A. R., Sali, A., Smith, L. J., Dobson, C. M. & Karplus, M. Understanding protein folding via free-energy surfaces from theory and experiment. *Trends Biochem. Sci.* **25,** 331–339 (2000).
10. Frieden, C. Slow transitions and hysteretic behavior in enzymes. *Annu. Rev. Biochem.* **48,** 471–489 (1979).
11. Flomenbom, O. *et al.* Stretched exponential decay and correlations in the catalytic activity of fluctuating single lipase molecules. *Proc. Natl Acad. Sci. USA* **102,** 2368–2372 (2005).
12. Lu, H. P., Xun, L. & Xie, X. S. Single-molecule enzymatic dynamics. *Science* **282,** 1877–1882 (1998).
13. English, B. P. *et al.* Ever-fluctuating single enzyme molecules: Michaelis-Menten equation revisited. *Nature Chem. Biol.* **2,** 87–94 (2005); erratum **2,** 168 (2006).
14. Herschlag, D. RNA chaperones and the RNA folding problem. *J. Biol. Chem.* **270,** 20871–20874 (1995).
15. Treiber, D. K. & Williamson, J. R. Exposing the kinetic traps in RNA folding. *Curr. Opin. Struct. Biol.* **9,** 339–345 (1999).
16. Chen, S.-J. & Dill, K. A. RNA folding energy landscapes. *Proc. Natl Acad. Sci. USA* **97,** 646–651 (2000).
17. Pan, J., Thirumalai, D. & Woodson, S. A. Folding of RNA involves parallel pathways. *J. Mol. Biol.* **273,** 7–13 (1997).
18. Zhuang, X. *et al.* Correlating structural dynamics and function in single ribozyme molecules. *Science* **296,** 1473–1476 (2002).
19. Tan, E. *et al.* A four-way junction accelerates hairpin ribozyme folding via a discrete intermediate. *Proc. Natl Acad. Sci. USA* **100,** 9308–9313 (2003).
20. Herschlag, D. Evidence for processivity and two-step binding of the RNA substrate from studies of J1/2 mutants of the *Tetrahymena* ribozyme. *Biochemistry* **31,** 1386–1399 (1992).
21. Bevilacqua, P. C., Kierzek, R., Johnson, K. A. & Turner, D. H. Dynamics of ribozyme binding of substrate revealed by fluorescence-detected stopped-flow methods. *Science* **258,** 1355–1358 (1992).
22. Ditzler, M. A., Rueda, D., Mo, J., Hakansson, K. & Walter, N. G. A rugged free energy landscape separates multiple functional RNA folds throughout denaturation. *Nucleic Acids Res.* **36,** 7088–7099 (2008).
23. Lindahl, T., Adams, A. & Fresco, J. R. Renaturation of transfer ribonucleic acids through site binding of magnesium. *Proc. Natl Acad. Sci. USA* **55,** 941–948 (1966).
24. Korennykh, A. V., Plantinga, M. J., Correll, C. C. & Piccirilli, J. A. Linkage between substrate recognition and catalysis during cleavage of sarcin/ricin loop RNA by restrictocin. *Biochemistry* **46,** 12744–12756 (2007).
25. Levinthal, C. Are there pathways for protein folding? *J. Chim. Phys.* **65,** 44–45 (1968).
26. Russell, R. *et al.* Exploring the folding landscape of a structured RNA. *Proc. Natl Acad. Sci. USA* **99,** 155–160 (2002).
27. Zhuang, X. *et al.* A single-molecule study of RNA catalysis and folding. *Science* **288,** 2048–2051 (2000).
28. Sattin, B. D., Zhao, W., Travers, K., Chu, S. & Herschlag, D. Direct measurement of tertiary contact cooperativity in RNA folding. *J. Am. Chem. Soc.* **130,** 6085–6087 (2008).
29. Russell, R. & Herschlag, D. Probing the folding landscape of the *Tetrahymena* ribozyme: commitment to form the native conformation is late in the folding pathway. *J. Mol. Biol.* **308,** 839–851 (2001).

Supplementary Information is linked to the online version of the paper at www.nature.com/nature.

Acknowledgements We thank T. H. Lee, B. Cui, H. Kim, W. Zhao and other current and former members of the Chu laboratory, and the Mabuchi laboratory, for technical assistance. We thank members of the Herschlag laboratory for discussions and comments on the manuscript. Financial support for this work was provided by US National Institutes of Health (NIH) programme project grant P01-GM-66275 and NIH grant GM49243, to D.H. We thank the Stanford Bio-X Program for fellowship support to S.V.S.

Author Contributions All authors contributed to the experimental design and writing of the manuscript. S.V.S. performed the experiments and M.G. and S.V.S. carried out data analysis.

Author Information Reprints and permissions information is available at www.nature.com/reprints. The authors declare no competing financial interests. Correspondence and requests for materials should be addressed to D.H. (herschla@stanford.edu).

METHODS

Reagents. We used the following enzymes. T7 RNA polymerase (His-tagged) was overexpressed in BL21 DE3 cells and purified by chromatography on Ni^{2+} resin; this was followed by dialysis against a storage buffer containing 20 mM phosphate buffer (pH 7.5), 100 mM NaCl, 10 mM DTT, 1 mM EDTA and 50% glycerol. Glucose oxidase (Type VII from *Aspergilius niger*, Sigma-Aldrich) and catalase (Roche) were used as supplied.

We used the following chemicals. D-glucose (SigmaUltra, 99.5%), guanosine 5′-monophosphate (Sigma-Aldrich, ≥99%), dNTPs (Fermentas, >98%), NTPs (Sigma, 95–99%), Trolox ((±)-6-hydroxy-2,5,7,8-tetramethylchromane-2-carboxylic acid, Aldrich, >97%), egg lecitin (Avanti Lipids) and cap-biotin phosphatidylethanolamine (Avanti Polar Lipids) were used without further purification.

Ribozyme preparation. L-16T2 ribozyme, which is a version of the L-21 ScaI ribozyme extended at the 5′-end with the sequence GGUUU and at the 3′-end with the sequence ACCAAAAUCAACCUAAAACUUACACA, was prepared by PCR amplification of a DNA template from a plasmid pT7L-21 with the extensions encoded on the primers. The ribozyme was prepared by a run-off *in vitro* transcription of the DNA template in conditions that minimize self-processing of the 5′-end (30 min at 30 °C with 4 mM $MgCl_2$ present). RNA was purified by denaturing polyacrylamide gel electrophoresis (8% of 29:1 acrylamide:bisacrylamide) and stored as a ~20 μM stock solution at −20 °C.

Oligonucleotide labelling. We purchased RNA oligonucleotides CCCUCdUA (dU, 2′-deoxyuridine), CCCUCmUAAACC (mU, 2′-methoxyuridine) and CCCmUCUAAACC, with 3′-amino modification from Dharmacon (now Thermo Scientific) and deprotected them according to manufacturer's instructions. We modified the 3′-amino groups with Cy3-NHS (Invitrogen) and purified labelled oligonucleotides from unlabelled and shorter oligonucleotides (present in synthetic oligonucleotides because of <100% coupling efficiency) by denaturing polyacrylamide gel electrophoresis (20% of 29:1 acrylamide:bisacrylamide). After purification, oligonucleotides were dissolved in distilled water and stored at −80 °C.

We purchased DNA oligonucleotide T2b (TGTGTAAGTTTTAGGTTGATTT TGGT) with 5′-biotin and 3′-amino modifications from Integrated DNA Technologies and labelled it with Cy5-NHS and purified it as described above.

Sample preparation. Solutions of L-16T2 ribozyme and T2b-Cy5 were mixed together (2:1 molar ratio; final concentration of RNA, 1 μM) in an annealing buffer (50 mM NaMES (pH 6.0), 200 mM NaCl) and annealed by heating at 95 °C for 3 min then cooling to 50 °C at 0.1 °C s^{-1}. We initiated folding by adding $MgCl_2$ to a final concentration of 10 mM. The ribozyme was folded for 30 min at 50 °C (ref. 30).

Oligonucleotide substrates were bound by mixing 2 μl prefolded L-16*T2b-Cy5 (1 μM) and 0.5 μl S-Cy3 (2 μM) in 50 mM NaMES (pH 6.0) and 10 mM $MgCl_2$, and incubating at room temperature (22 °C) for 10 min. We diluted ternary complex L-16*T2b-Cy5*S-Cy3 to a final concentration of 30–100 pM for deposition on the slides.

Quartz slides (G. Finkenbeiner) were coated with biotinylated bovine serum albumin (Sigma; 1 mg ml^{-1} for 10 min), washed thoroughly with 50 mM NaMOPS (pH 7.0), then coated with streptavidin (Sigma; 0.1 mg ml^{-1} for 10 min) and washed thoroughly with 50 mM NaMOPS (pH 7.0) and, finally, with 50 mM NaMES (pH 6.0) and 10 mM $MgCl_2$.

Ternary complexes L-16*T2b-Cy5*S-Cy3 were deposited over the coated slides for 10 min and then thoroughly washed with 50 mM NaMES and 10 mM $MgCl_2$. We performed measurements of docking in a standard buffer containing 50 mM NaMES (pH 7.0), 10 mM $MgCl_2$, 100 mM NaCl and an oxygen scavenging system (100 units ml^{-1} glucose oxidase, 1,000 units ml^{-1} catalase, 10 mM D-glucose and 2 mM Trolox). The cleavage buffer was the same, except we used 50 mM NaMOPS (pH 8.1) instead of NaMES, and added 1 mM guanosine 5′-monophosphate. Higher pH accelerates cleavage, thereby facilitating measurement of the chemical step, and has been shown to have no effect on docking[30].

TIRF microscope and data acquisition. A diode-pumped solid-state green laser (532 nm; Gem, Laser Quantum) and a red laser (635 nm; Hitachi HL6344G diode; maximum power, 10 mW) were combined using dichroic mirrors and focused through a prism onto a sample contained in a flow cell made from a quartz slide and a cover slip glued together using double-sided tape. Laser beams entered the prism at an angle ensuring total internal reflection of the exciting light. We collected images using a ×60 water-immersion Nikon objective (numerical aperture, 1.2), filtered through a 550-nm long-pass filter (Chroma Technology) to remove scattered excitation light and chromatically separated using dichroic mirrors (635-nm cut-off) into a 'green' image and a 'red' image. We focused the 'green' image, filtered through a 580/30-nm band-pass filter, and the 'red' image, filtered through 670/30-nm band-pass filter, onto the left and right halves of a back-illuminated charge-multiplying charge-coupled device (CCD) (Cascade:128+, Photometrics, Roper Scientific), respectively. Full CCD images (128 × 128 pixels) were read out in 40-ms frames with a conversion gain of 3 and multiplication gain of 3,500. The red laser was typically switched on only for the first 0.5 s of data acquisition and at the end of data acquisition to determine which of the molecules had fluorescently active Cy5 dye. We adjusted the intensity of the green laser to achieve an average signal-to-noise ratio of >5, which typically required a power of ~20 mW at the laser aperture.

Data analysis and simulations. To record FRET data, we determined the positions of spots of interest within each data acquisition 'movie' by averaging the first 30 frames and finding pixels on the 'red' side of the CCD with an intensity that exceeded a certain threshold (typically a threshold of 5σ, where σ is the standard deviation of the background fluorescence). The corresponding positions on the 'green' side were determined by applying linear offsets (determined independently from images of fluorescent beads that are visible on both sides of the CCD) and further refining by the 'affine' algorithm of MATLAB. The local (7 × 7 pixel) background was subtracted from each spot for each frame. Time traces of the fluorescent intensity (I) of Cy3 and the Cy5 for each spot were recorded and used to calculate a FRET trace (for each frame, FRET equals $I_{red}/(I_{green} + I_{red} - I_{cross\text{-}talk})$). The value of the cross-talk (intensity in the red channel arising from Cy3 fluorescence because of imperfect chromatic separation) was determined by measuring the 'red' intensity for molecules that contain only Cy3.

To identify molecules, for each spot we visually screened Cy 3 and Cy5 traces to determine whether they corresponded to a single RNA molecule, and accepted that they did if they met the following criteria: (1) they exhibit single-step photobleaching (the fluorescence intensity goes to the background level within one frame); (2) they have a stable signal (the average fluorescence intensity along the trace is constant; it does not gradually decrease or increase); (3) they have a normal signal strength (fluorescence intensity is within a factor of two of the average; very dim and very bright spots were rejected); (4) Cy5 is fluorescent ('red' fluorescence is detected when the red laser is switched on at the beginning and the end of data acquisition; if Cy5 was fluorescent at the beginning, but not at the end, of data acquisition, the trace was truncated at the last frame where Cy5 was fluorescent).

We measured the thermodynamics and kinetics of individual models in the following way. FRET traces for >95% of the molecules (defined by the above criteria) displayed fluctuations between two FRET levels, low FRET (0.35) and high FRET (0.95), respectively corresponding to undocked and docked state, as described previously[28]. Transitions between FRET levels were identified by a standard thresholding method. The threshold was set at 0.7. On average, each trace contained ~30 transitions, allowing precise estimates of the rate constants. Rate constants were determined by creating histograms of dwell times in the docked state (to measure k_{dock}) and in the undocked state (to measure k_{undock}), and fitting histograms to a sum of exponentials. For most traces, the histograms were well described by a single exponential decay. Equilibrium constants between docked and undocked conformations were determined as a ratio of the total time spent in docked (t_{dock}) and in undocked (t_{undock}) states: $K_{dock} = t_{dock}/t_{undock}$. From this, the free energy of docking was calculated as: $\Delta G_{dock} = -RT \times \ln K_{dock}$, where R is the molar gas constant and T denotes temperature.

Because of photobleaching, each molecule can be observed for only a limited time, $t_{life} \approx 1/k_{bleach}$, which makes the value of ΔG_{dock} calculated for each trace a random parameter distributed around a true mean. For a trace that fluctuates between two FRET levels with a forward rate constant k_{dock} and a reverse rate constant k_{undock}, the width of the ΔG_{dock} distribution depends only on k_{dock}, k_{undock} and k_{bleach}. To estimate the extent of broadening, we first measured the distribution of trace lengths and from it calculated the photobleaching rate constant $k_{bleach} = 0.03\ s^{-1}$ (Supplementary Fig. 1). We then performed numerical simulations of the ΔG_{dock} distribution for a broad range of k_{dock} and k_{undock} values, keeping k_{bleach} fixed. For each pair of parameters k_{dock} and k_{undock}, 1,000 traces were simulated by a lab-written program in MATLAB, ΔG_{dock} for each trace was calculated as above and histograms were fitted using a Gaussian distribution. As the results of the simulations demonstrate (Supplementary Fig. 2), for any combination of the rate constants k_{dock} and k_{undock} that were experimentally measured, the width ($w = 2\sigma$, where σ is the standard deviation) of the ΔG_{dock} distribution is small (typically ≤0.3 kcal mol^{-1}) in comparison with the experimentally observed width (~1 kcal mol^{-1}). Comparing the results of these simulations with the experimental data, we see that a single population of molecules, characterized by a single set of ΔG_{dock}, k_{dock} and k_{undock} values, cannot account for the experimentally observed width of the ΔG_{dock} distribution. As illustrated in Supplementary Fig. 3, at least six distinct populations, each with different ΔG_{dock}, k_{dock} and k_{undock} values, are required to account for the full width of the distribution. These six conformations should be considered a minimum number of coexisting conformations that can be determined given the limited resolution of ΔG_{dock} that is imposed, ultimately, by photobleaching.

Cleavage experiments. First, docking was observed for 20 s essentially as described above. Then the laser was switched off and the cleavage buffer containing 1 mM guanosine 5′-phosphate was flowed through the sample at $\sim$40 μl s^{-1} for 5 s. Immediately after buffer replacement, and then subsequently after several time intervals, we switched the laser on for 2 s at a time (to allow confident detection of remaining molecules while limiting photobleaching) and recorded images of the slide. Fluorescent spots were defined as molecules with the uncleaved substrates if they fulfilled the criteria of signal stability and intensity (criteria 2 and 3 above). Control experiments establishing that the rate of substrate disappearance in the absence of guanosine is negligibly small were performed in exactly the same way, but omitting guanosine 5′-phosphate from the cleavage buffer.

Unfolding/refolding experiments. We performed the experiments in two steps: in the first step, docking was observed for 20 s essentially as described above. Then the laser was switched off and the unfolding buffer containing 12 mM EDTA was flowed through the sample at $\sim$40 μl s^{-1} for 5 s. Unfolding was ensured by quickly switching the laser on and verifying that all molecules were in low FRET state. After 1 min in EDTA, the standard folding buffer was flowed back in and docking was observed for 20 s. Docking equilibria for each molecule before and after unfolding were measured as described above. To test whether molecules changed their docking behaviour, we calculated the uncertainty of measuring the docking equilibrium as the width of the simulated distribution (Supplementary Fig. 2). The *P* values were calculated using a right-tailed chi-squared variance test implemented in MATLAB with the null hypothesis that the difference between docking equilibria before and after unfolding is equal to, or smaller than, the uncertainty in the measurement.

30. Narlikar, G. J., Bartley, L. E., Khosla, M. & Herschlag, D. Characterization of a local folding event of the *Tetrahymena* group I ribozyme: effects of oligonucleotide substrate length, pH, and temperature on the two substrate binding steps. *Biochemistry* **38,** 14192–14204 (1999).